Engineered Science
DOI: https://dx.doi.org/10.30919/es1958

Bioactive *Papaver somniferum* Extract-Loaded Polyvinyl Alcohol Hydrogels for Enhanced *in vivo* Wound Healing Applications

Faiza Tariq,[1] Adeeb Shehzad,[1,2,*] Mazhar Ul-Islam,[3] Abdullah Al-Saidi,[3] Sehrish Manan,[4,5] Fazli Subhan,[6] Fanar Hamad Alshammari,[7] Guang Yang[8,*] and Muhammad Wajid Ullah[4,5,*]

Abstract

This study aims to develop a bioactive hydrogel composed of *Papaver somniferum* extract (PSE) and polyvinyl alcohol (PVA) for enhanced *in vivo* wound healing applications. The pod-derived PSE was incorporated at varying concentrations (0.25%, 0.5%, and 1.0% w/v) into the PVA matrix *via ex situ* impregnation to form the PSE-PVA hydrogel. Scanning electron microscopy (SEM) showed a smoother, more organized texture and fiber-like morphology of the PSE-PVA hydrogel. Fourier transform infrared (FTIR) analysis confirmed chemical interactions between PSE and PVA components. The swelling behavior of the PSA-PVA hydrogels showed a concentration-dependent increase in water absorption, reaching a maximum swelling ratio of 86% after 250 min at 1.0% PSE concentration. Antibacterial testing through disc diffusion assay demonstrated formation of clear inhibition zones measuring 16.5 mm against *Escherichia coli* and 15.2 mm against *Staphylococcus aureus* at 1.0% PSE-PVA concentration. *In vivo* wound healing studies showed that the PSE-PVA hydrogel achieved the highest wound closure, reducing wound size by 95% by day 24—compared to 78% with PSE alone and 20% in the untreated control group. Histological analysis showed that wounds treated with 1% PSE-PVA hydrogel exhibited rapid epidermal regeneration, re-epithelialization and granulation. Histology studies confirmed the early formation of hair follicles and sebaceous glands in treated tissues. These findings suggest that PSE-PVA hydrogels are promising candidates for multifunctional wound dressings due to their biocompatibility, antibacterial efficacy, and ability to accelerate tissue regeneration.

Keywords: Hydrogel; *Papaver somniferum*; Antibacterial; Wound healing.
Received: 14 September 2025; Revised: 29 November 2025; Accepted: 15 December 2025
Article type: Research article.

1. Introduction

The skin serves as the primary protective barrier of the body, shielding against environmental toxins while regulating essential physiological processes and providing defence mechanisms. Skin repair after injury involves multiple complex processes that stimulate tissue regeneration and promote healing.[1,2] The main goal of wound healing is to restore tissue integrity and maintain homeostasis.[3,4] This natural healing process occurs in four distinct, yet overlapping phases: haemostasis, inflammation, proliferation, and remodelling.[5] Wound healing is one of the most intricate biological processes, requiring precise coordination of various cell types at specific times and locations. Each cell type plays a key role in haemostasis, inflammation, cell growth, re-epithelialization, and remodelling.[6] Cellular events like mitosis govern this healing process, but delays can lead to complications.[7] Conventional wound dressings, such as patches and gauze, are often inadequate and, in some cases, may worsen the condition by causing additional tissue damage.[8] These limitations highlight the need for innovative wound dressings that not only protect wounds from microbial, chemical, and physical damage but also support cell adhesion and proliferation.[9] Moreover, incorporating bioactive substances is essential to accelerate healing.[10,11] Consequently, the development of advanced dressing materials has become a critical focus in modern medical technology.

Hydrogels have emerged as one of the most effective materials for modern wound dressings, owing to their

[1]*Department of Biomedical Engineering and Sciences, School of Mechanical and Manufacturing Engineering, National University of Sciences and Technology, Islamabad, 44000, Pakistan*
[2]*Biodiversity Unit, Research Centre, Dhofar University, Salalah, 211, Oman*

remarkable moisture retention and bioactivity properties.[12] These materials facilitate oxygen permeability, absorb exudates, and maintain a moist environment, all of which contribute to improved wound healing.[13] Additionally, hydrogel adhesives serve to prevent bacterial colonization and promote gaseous exchange, which helps inhibit the growth of anaerobic bacteria. The incorporation of encapsulated antibiotics within the polymeric network of hydrogels further enhances their antibacterial properties.[14,15] Wound dressings made from materials with intrinsic antibacterial characteristics are especially desirable. In comparison to traditional dressings, modern hydrogel-based alternatives are preferred due to their ability to deliver bioactive molecules in a controlled and targeted manner, leading to better therapeutic outcomes.[16] Among the various types of hydrogels, polyvinyl alcohol (PVA) hydrogels have gained significant attention for wound healing applications. This is due to their excellent biocompatibility, chemical stability, ease of synthesis, and tunable properties.[17] PVA hydrogels are typically prepared by dissolving PVA in water, followed by physical crosslinking through hydrogen bonding interactions between the hydroxyl groups in the polymer structure.[18,19] The characteristics of the resulting hydrogel are influenced by several factors, including the molecular weight, degree of hydrolysis, crosslinking method and conditions, and the incorporation of other compounds into the hydrogel. The number of freeze-thaw cycles during crosslinking can also significantly affect the mechanical strength, elasticity, and swelling properties of the hydrogel. Furthermore, blending PVA with other polymers or bioactive molecules can enhance its functionality, such as improving antimicrobial activity or supporting tissue regeneration.[20-22]

Some plants, containing bioactive ingredients, are considered ideal candidates for wound healing due to their simplicity and affordability.[23] Among these, the opium poppy (*Papaver somniferum*) has a long history of traditional use in wound healing and other medicinal applications.[24,25] In recent years, various plant-based (*Aloe vera*, *Moringa oleifera*, *Centella asiatica*) and polymeric biomaterials have been explored for wound healing applications due to their biocompatibility, antibacterial properties, and ability to promote tissue regeneration.[26] Adding to this growing field of research, this study investigates the unique therapeutic potential of *P. somniferum* extract. Unlike many other botanical sources, *P. somniferum* contains pharmacologically active alkaloids such as morphine, codeine, thebaine, noscapine, and papaverine, which provide a rare combination of analgesic, anti-inflammatory, antispasmodic, and antimicrobial properties.[27-30] Morphine and codeine, for example, exhibit potent pain-relieving properties and have been reported to promote granulation tissue formation and reduce inflammatory response.[31] Papaverine has demonstrated vasodilatory and antimicrobial effects, while noscapine has shown anti-inflammatory and antioxidant activities in various wound models.[32] The presence of such compounds in the extract may synergistically contribute to enhanced wound healing and infection control when incorporated into the hydrogel system. Previous research has also demonstrated antimicrobial, antioxidant, anti-cancer, and antidiabetic effects associated with *P. somniferum* extracts (PSE).[33] For instance, morphine, a key alkaloid derived from the opium poppy, has been shown to enhance wound healing by promoting angiogenesis, collagen production, and epithelialization.[34] These findings suggest that PSE extracts can accelerate wound closure, improve collagen formation, and reduce oxidative stress and inflammation.

This study focuses on developing biodegradable hydrogel membranes for wound dressing applications. While PVA-based nanocomposite films have been previously explored for various uses, including wound dressings,[35,36] this study introduces a novel approach by incorporating a plant extract prepared in a water-methanol mixture. The hydrogel membranes were comprehensively characterized through SEM, FT-IR, and moisture retention capacity evaluations. Additionally, the study thoroughly investigated the antibacterial properties, wound-healing potential, and tissue regeneration capabilities of the plant extract-based hydrogel, emphasizing its potential as an advanced material for wound healing applications.

2. Materials and methods

2.1 Materials

Parts of *P. somniferum* (pods) were collected from the Khyber Pakhtunkhwa (KP) province of Pakistan. Polyvinyl alcohol (PVA; average molecular weight ~89,000–98,000 g/mol; 98–99% hydrolyzed) was obtained from Daejung Chemicals (South Korea). Ethanol (99.8%), methanol (99.9%), glycerol, and formaldehyde were sourced from Sigma-Aldrich (St. Louis, MO, USA).

2.2 Preparation of *P. somniferum* extract

P. somniferum pods (*50 g)* were collected, washed with distilled water, and dried in the shade to prevent photochemical reactions. The dried pods were then ground into a fine powder and mixed with a 1:3 methanol-water solution (final volume 300 mL). The mixture was stirred for 7 days at 25 °C. After filtration to remove solid particles, the extract was concentrated using a rotary evaporator (REV-2000AX) at 153 rpm and 60 °C to remove the methanol. The

[3]*Department of Chemical Engineering, College of Engineering, Dhofar University, Salalah, 211, Oman*

[4]*Department of Pulp & Paper Engineering, College of Light Industry and Food Engineering, Nanjing Forestry University, Nanjing, 210037, China*

[5]*Department of Biosciences, University of Wah, Quaid Campus, Wah Cant, 47010, Pakistan*

[6]*Department of Biological Sciences, National University of Medical Sciences, Rawalpindi, 46000, Pakistan*

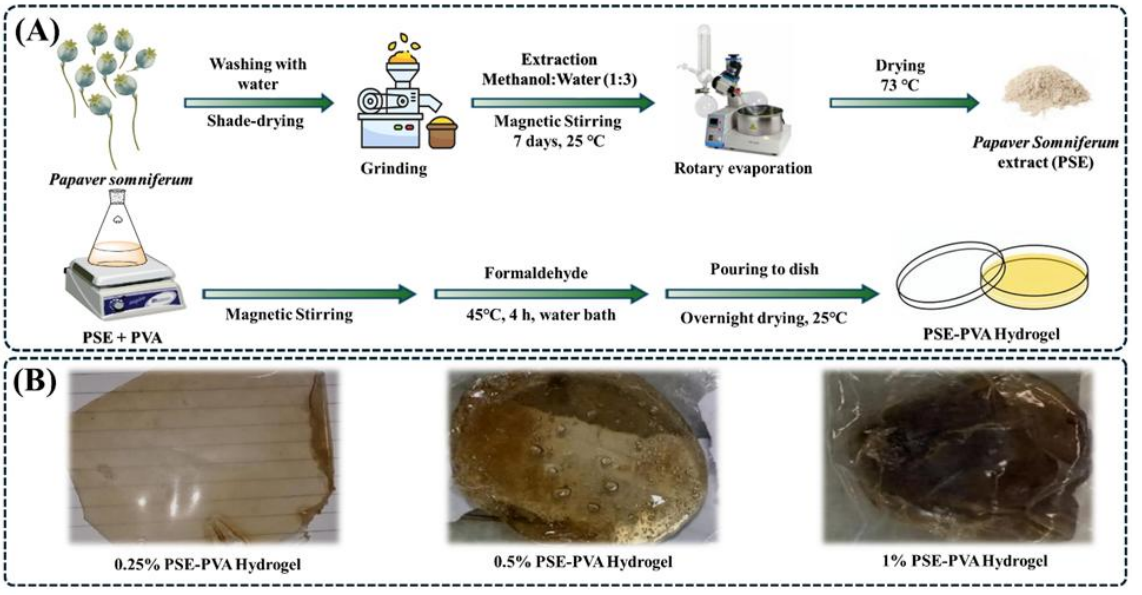

Fig. 1: (A) Schematic representation of the process for extracting *P. somniferum* extract (PSE) and synthesizing PVA and PSE-PVA hydrogels. The process begins with the extraction of PSE from pods using a milling machine, followed by refinement using a rotary evaporator. The PSE extract was then combined with PVA, and the resulting mixture underwent a controlled process to form PSE-PVA hydrogels. (B) Photographs displaying hydrogels with varying concentrations of PSE, including 0.25%, 0.5%, and 1%, showing differences in texture and appearance based on the PSE concentration.

remaining extract was further dried in a water bath at 73 °C to remove any residual water, cooled, and stored at 4 °C for future analysis. The dry weight of the extract was recorded to determine the extraction yield, and a stock solution was prepared for further use. A schematic illustration of the preparation of PSE, following a previously reported protocol,[37] with some modifications, is shown in Fig. 1.

2.3 Preparation of PSE-PVA hydrogels

First, a PVA hydrogel membrane was prepared using a method described in the literature.[38] Briefly, 5 g of PVA at a concentration of 10 wt.% was dissolved in 50 mL of distilled water. The solution was heated to 70 °C and stirred continuously for 2 h to ensure complete dissolution, resulting in a transparent solution. Next, 2 mL of formaldehyde (37% aqueous solution) was added as a crosslinker, and 1.0 mL of glycerol was incorporated as the plasticizer to enhance membrane flexibility and the mixture was stirred gently to ensure uniform incorporation of all components. Next, PVA hydrogel membranes impregnated with plant extract (*i.e.*, PSE-PVA hydrogels) were prepared by adding various concentrations of PSE (1%, 0.5%, and 0.25%) to 12 mL of the PVA solution and stirred for 1 h. These concentrations were prepared as w/v (weight of dried extract per total volume of solution), and the final concentration of PSE in each hydrogel formulation corresponded to 0.25%, 0.5%, or 1.0% relative to the 12 mL volume of the PVA solution. The selected concentrations of PSE (0.25%, 0.5%, and 1.0% w/v) were based on preliminary optimization studies aimed at optimizing extract solubility, formulation stability, and antibacterial activity. These concentrations provided effective integration into the PVA matrix without compromising hydrogel integrity and remained non-toxic. A 2.0 mL formaldehyde was then added as a cross-linker, and the mixtures were heated in a water bath at 45 °C for 4 h. The solutions were poured into petri dishes to form membranes and left to dry overnight at room temperature. The resulting flexible PSE-PVA membranes were carefully separated, stored in plastic bags, and refrigerated for six days. A schematic illustration of the preparation of PSE-PVA hydrogel membranes is shown in Fig. 1A and B.

2.4 Characterization

The characterization of PSE-PVA hydrogel membranes involved a comprehensive evaluation of their physical, structural, and swelling properties to assess their performance and potential applications. The physical properties of the biocomposite scaffolds, including color, texture, and surface integrity, were thoroughly examined. The dimensions of the scaffolds were accurately measured using a digital Vernier micrometer to ensure consistency. These measurements are presented in Table 1, while images of hydrogels in Fig. 1

[7]*Department of Biological Sciences, College of Sciences, Northern Border University, Arar, 73213, Saudi Arabia*
[8]*Department of Biomedical Engineering, College of Life Science and Technology, Huazhong University of Science and Technology, Wuhan, 430074, China*
[*]*Email*: ashehzad@du.edu.om (A. Shehzad),
gyang-hust@hust.edu.cn (G. Yang),
wajid kundi@njfu.edu.cn (M. W. Ullah)

Table 1: Physical assessment of synthesized hydrogels.

Hydrogel label	Color	Thickness (mm)	Texture
0.25% PSE-PVA	Pale brown	1.5 ± 0.1	Smooth
0.50% PSE-PVA	Honey brown	2.2 ± 0.1	Smooth
1.00% PSE-PVA	Dark brown	3.0 ± 0.1	Irregular

provide their visual representation for clarity and comparison. The swelling behavior of the PSE-PVA hydrogel was assessed using the gravimetric method to measure its water absorptivity. Briefly, pre-weighed samples were immersed in distilled water at 25 °C for 4 h until equilibrium swelling was achieved. After gently wiping off any excess surface water, the swollen samples were weighed. The swelling ratio was calculated using Eq. (1).

$$\text{Swelling ratio (\%)} = \frac{(W_s - W_d)}{W_d} \times 100 \qquad (1)$$

where W_s and W_d represent the weights of the swollen and dried gels, respectively. Measurements were performed in triplicate to ensure the accuracy of the results.

The structural morphology of both PSE and PSE-PVA hydrogel was observed through the scanning electron microscope (SEM, JEOL JSM-64900). Additionally, the cross-sectional view of the PSE-PVA hydrogel was also observed under SEM. Prior to SEM observation, the freeze-dried samples were coated with osmium tetroxide (OsO_4) using a VD HPC-ISW osmium coater (Tokyo, Japan), and a brass holder was used to secure the samples in the device. Fourier transform infrared (FTIR) spectra of the freeze-dried PSE and PSE-PVA membrane were recorded using a PerkinElmer FTIR spectrophotometer (Spectrum TM100, GX & Autoimage, USA), equipped with a KBr beam splitter and a mid-IR detection range of 4000–400 cm^{-1}.

2.5 *In vitro* antibacterial activity assay

Antibacterial activity of the PSE-PVA hydrogels was evaluated against three standard bacterial strains: *Staphylococcus aureus* ATCC6538, *Escherichia coli* ATCC8739, *Klebsiella pneumoniae* KP6870155, and *Acinetobacter baumannii* AB6870155, obtained from a certified microbial culture bank. These strains were selected due to their clinical relevance in wound infections. Each bacterial strain was revived on its respective culture medium and incubated at 37 °C for 18–24 h: *E. coli* on Luria broth, *S. aureus* on MacConkey agar, and *A. baumannii* and *K. pneumoniae* on nutrient agar. Following incubation, a single colony from each strain was inoculated into 5 mL of Mueller-Hinton broth and incubated for 4 h at 37 °C. The bacterial suspension was then standardized to 0.5 McFarland turbidity (approximately 1 × 10^8 CFU/mL) using a turbidometer. Antibacterial susceptibility testing was conducted using the disc diffusion method, following standard procedures.[39] The antibacterial activity of PSE and PSE–PVA hydrogels, in both dry and wet forms, was assessed against each bacterial strain. Standardized bacterial suspensions were uniformly spread onto Mueller-Hinton agar plates. After the plates were allowed to dry for 15 min, they were used to test antibacterial activity. The plates were then incubated overnight at 37 °C for 24 h, and the antibacterial activity was assessed by measuring the zone of inhibition around each disc.

2.6 Full-thickness skin wound model

This study was carried out in accordance with relevant guidelines and received approval from the Biosafety and Bioethics Committee at the National University of Science and Technology, Islamabad, Pakistan. All procedures adhered to the ARRIVE guidelines (https://arriveguidelines.org) and followed the principles of the 3Rs (replacement, reduction, and refinement). Male mice, aged 5–6 weeks and weighing approximately 25 g, were obtained from the Atta-ur-Rehman School of Biological Sciences Animal House. The mice were randomly assigned to three groups (n = 3 per group): Group 1 (control), Group 2 (PSE extract), and Group 3 (PSE-PVA hydrogel). After anesthesia, the hairs on the backs of the mice were shaved, and an 8 mm full-thickness skin wound was created using a hole punch. The respective treatments were then applied to the wound sites according to the group assignments. Throughout the 24-day experimental period, the applied dressings were replaced if they became visibly detached or contaminated, in accordance with ethical animal care guidelines to minimize handling stress and disturbance to the healing process.

2.7 Wound healing

The morphological changes at the wound site were documented using a digital camera on days 1 and 24 post-treatment. Photographic images were taken to visually assess the healing process. Wound healing was further evaluated by measuring the wound area and assessing contraction. The wound dimensions were quantified using a scale to determine the extent of healing, providing a clear indication of tissue regeneration and wound closure over time.

2.8 Haematoxylin and eosin staining and wound healing analysis

Histological analysis was conducted to evaluate cellular and molecular changes during wound healing. Wound tissue samples were collected and fixed in 4% paraformaldehyde for 1 h to preserve tissue morphology and prevent cellular

degradation. The fixed samples were then dehydrated through a series of ethanol solutions, embedded in paraffin wax, and sectioned for further analysis. Haematoxylin and eosin (H&E) staining was used to visualize the tissue architecture, with nuclei appearing blue and cytoplasm pink. The stained sections were examined under a microscope, and various software programs were employed to assess key aspects of wound healing, including cell density, collagen deposition, and angiogenesis.

2.9 Statistical analysis

Data are presented as the mean ± standard deviation (SD) from three independent experiments. Statistical analysis was performed using SPSS, with the Student's *t*-test and one-way or two-way analysis of variance (ANOVA) applied as appropriate. Mean differences were considered statistically significant at $*p \leq 0.05$.

3. Results and discussion

3.1 Structural morphology of PSE-PVA composite hydrogel

The SEM micrographs in Fig. 2 demonstrate the morphological differences between pure PSE and its composite hydrogel with PVA (*i.e.*, PSE-PVA) at various magnifications. Pure PSE hydrogel at X500 magnification (50 µm scale bar) displays a relatively rough surface and porous morphology with irregular and undefined structures, indicating a heterogeneous texture. As the magnification increases to X1000 (10 µm scale bar), the surface becomes more compact and the structures appear finer. This form interconnected microstructures, revealing self-assembly processes during drying that form irregular, folded structures. At X2500 magnification (10 µm scale bar), a more intricate and detailed surface texture emerges, showing the formation of smaller aggregates or nanostructures with smoother regions bounded by clustered microdomains within the PSE. This could be attributed to the natural tendency of plant extract-based hydrogels to form nanoscale aggregates due to the complex interactions of bioactive compounds in the plant extract.[23] The formation of such structures could influence the viscosity, porosity, and bioactivity of the hydrogel. In contrast, the addition of PVA resulted in a smoother, more organized surface. At X1000 magnification (10 µm scale bar), the surface appears much smoother and more uniform than in the pure PSE hydrogel, indicating that the addition of PVA helps to create a more consistent surface texture with minimal aggregation or defects. The PVA component likely plays a role in stabilizing the hydrogel structure, reducing the roughness observed in pure PSE. At X2500 magnification (10 µm scale bar), the cross-section view shows finer, more organized layered structures with distinct ridges and striations, suggesting that PVA contributes to the creation of a denser and more structured hydrogel network. This also indicates the effective impregnation of PSE in the PVA matrix. The layered arrangement proposes the formation of a stable hydrogel-like network, suggesting the mechanical integrity of the composite. The PSE-PVA hydrogel at X1000 magnification (10 µm scale bar) reveals elongated, fiber-like structures within the composite hydrogel, possibly indicating that PVA aids in the alignment of components during hydrogel formation, leading to the development of microfibers or threads. The formation of fiber-like structures in the PSE-PVA composite hydrogel is an important feature. Fiber formation in polymer-based hydrogels is well-documented in the literature, particularly in the context of PVA, where the polymer can lead to the alignment of the hydrogel components, forming elongated and fibrous structures.[20,40] This phenomenon has been attributed to the ability of PVA to organize the hydrogel matrix during the drying or gelation process, aligning the polymer chains in a way that supports fiber formation. In the case of the PSE-PVA composite hydrogel, these fiber-like structures could be beneficial for various applications. Such fibers in hydrogels can improve their mechanical properties, increase surface area, and enhance controlled release characteristics.[29,41] Thus, the

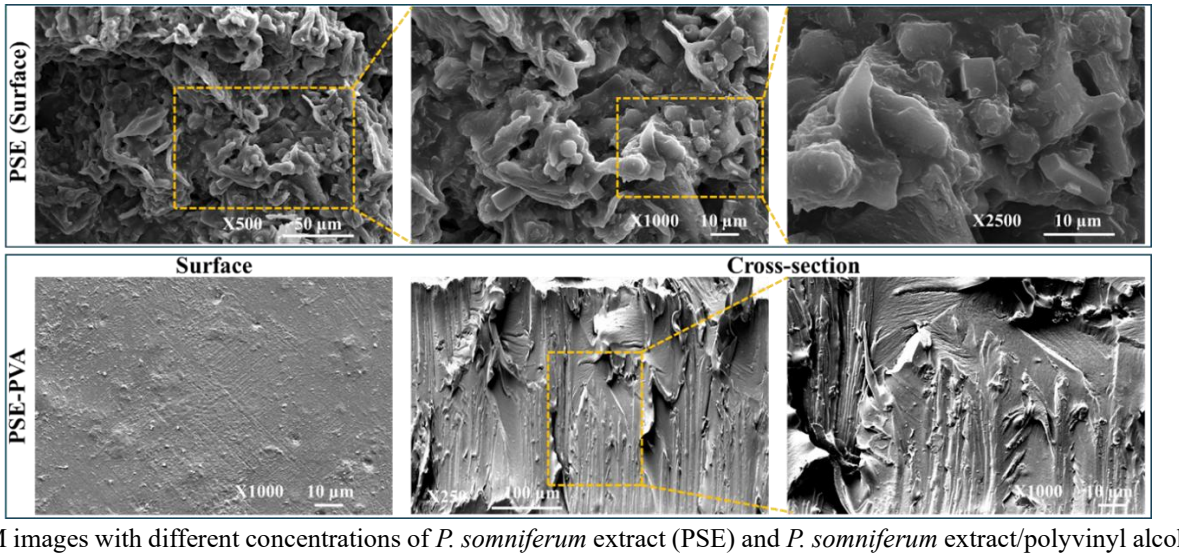

Fig. 2: SEM images with different concentrations of *P. somniferum* extract (PSE) and *P. somniferum* extract/polyvinyl alcohol (PSE-PVA) composite hydrogel.

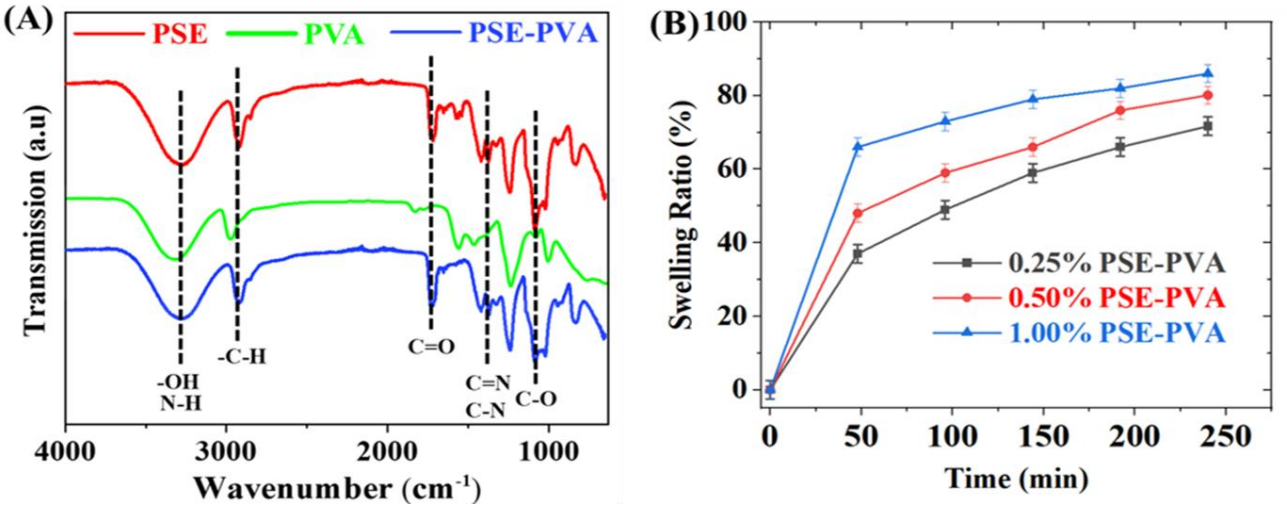

Fig. 3: (A) FTIR spectra of *P. somniferum* extract (PSE) and *P. somniferum* extract/polyvinyl alcohol (PSE-PVA) composite hydrogel. (B) Swelling performance of PSE extract and PSE-PVA hydrogels with varying concentrations of PSE (0.25%, 0.50%, and 1.0%).

PVA-PSE composite could offer enhanced performance for applications such as drug delivery systems or wound healing, where controlled and sustained release is desired. These findings suggest that the incorporation of PVA into the PSE formulation significantly altered the surface morphology and structure of the composite hydrogel. While pure PSE displayed an irregular and rough surface, the PSE-PVA composite exhibited a smoother, more organized surface, with the potential formation of microstructural fibers. This indicates that PVA not only stabilized the PSE hydrogel but may also improve the mechanical and structural properties of the composite material. The differences in surface texture and the formation of fibers in the composite hydrogel suggest that the PVA-PSE interaction may enhance the potential of hydrogel for applications such as controlled release or biomedical uses, where stability and structure are critical.

3.2 Chemical structure of PSE-PVA hydrogel

The comparative FTIR spectra of PSE and PSE-PVA composite hydrogel showed altered spectral characteristics (Fig. 3A), indicating chemical interaction between plant extract and polymer backbone. This chemical interaction provides insights into the functionalization and stability of the composite material. The characteristic absorption peaks of PVA appeared at 3286 cm^{-1} (O–H stretching), 2930 cm^{-1} (C–H stretching), and 1095 cm^{-1} (C–O stretching). In the FTIR spectrum of PSE, the broad absorption band around 3300 cm^{-1} is characteristic of the O-H stretching vibration from hydroxyl groups, which is commonly observed in alcohols and phenols. The presence of this peak indicates that PSE contains phenolic compounds or alcohols, which are typically bioactive components of plant extracts.[42] Similarly, the C-H stretching vibration near 3000 cm^{-1} further suggests the presence of alkyl groups, which is common in many organic plant-derived compounds.[43] The peak around 1600 cm^{-1} corresponding to C=O stretching confirms the presence of carbonyl-containing compounds, likely from organic acids, esters, or aldehydes within the plant extract.[44] Peaks in the region around 1200–1000 cm^{-1} indicate the presence of C-O stretching, which could correlate to alcohols, esters, or ethers in the plant components.[45] The introduction of PVA into the PSE extract resulted in a noticeable change in the FTIR spectrum of the PSE-PVA composite hydrogel, confirming the successful interaction between PSE and PVA. The broad -OH stretching peak around 3300 cm^{-1} became less obvious and shifted marginally, indicating formation of hydrogen bonding between the hydroxyl groups of PSE and PVA.[46] The C-H stretching vibration around 2925 cm^{-1} remained but became slightly reduced in intensity, indicating integration of PSE into the PVA matrix. The C=O stretching peak around 1650 cm^{-1} appeared more pronounced in the PSE-PVA composite, representing the retention of carbonyl groups from PSE after incorporation into the PVA matrix. The appearance of new peaks around 1550–1450 cm^{-1}, corresponding to C=N and C-N vibrations, respectively, suggests the potential Schiff base formation or additional interactions between PSE phytochemicals and PVA during the gelation process.[47] The C-N stretching vibration observed near 1250 cm^{-1} further suggests that the PSE-PVA composite hydrogel contains nitrogen-related interactions, possibly due to the interaction of nitrogen-containing compounds in PSE within the PVA matrix. The shifts in peak positions and the intensities of these bands suggest that chemical interactions, such as hydrogen bonding and covalent linkages, might have occurred between the functional groups in PSE (such as hydroxyl and carbonyl groups) and those in PVA (such as the carbonyl and hydroxyl groups). These interactions could play a significant role in the physical properties of the composite material, including its stability, hydrogel formation, and potential bioactivity. The changes observed in the FTIR spectra of the composite suggest that PVA not only provides a structural matrix but also influences the interaction dynamics of the active components in PSE. Overall, FTIR analysis confirms that the PSE-PVA composite material is chemically distinct from the pure PSE

extract, highlighting the important interactions that occur between the plant extract (*i.e.*, PSE) and the polymer (*i.e.*, PVA).

3.3 Swelling behavior of PSE-PVA hydrogels

Hydrogels are three-dimensional cross-linked polymers that can absorb and retain significant amounts of water or biological fluids, making them well-suited for biomedical applications.[48] Their swelling behavior, which is a key characteristic, is affected by factors such as the presence of hydrophilic groups, cross-linking density, network elasticity, and external conditions like pH and temperature.[49] Fig. 3B illustrates the swelling performance of PSE and its composite hydrogel with PVA at varying concentrations of PSE (0.25%, 0.50%, and 1.00%) over a period of 250 min. All three PSE-PVA composite hydrogels exhibited an increase in swelling ratio over time, with higher concentrations of PSE resulting in faster and more extensive swelling. The 1.0% PSE-PVA composite hydrogel showed the highest swelling ratio, reaching nearly 86% after 250 min, indicating that a higher concentration of PSE significantly enhanced the swelling capacity of the PSE-PVA hydrogel. The 0.50% PSE-PVA composite reached around 70% swelling, while the 0.25% PSE-PVA composite exhibited the slowest swelling behavior, reaching a final swelling ratio of just under 50%. As time progressed, the swelling of the PSE-PVA composites became more pronounced, but the rate of swelling slowed as equilibrium was approached. The swelling behavior suggests that PSE concentration plays a critical role in enhancing the water-absorbing properties of the hydrogel, with the 1.0% PSE-PVA hydrogel swelling faster and more extensively than the lower concentrations. This could be due to the increased number of hydrophilic functional groups in the PSE, which may interact with water molecules, allowing for a greater volume of absorption. The swelling performance of the PSE-PVA hydrogels might also be influenced by the nature of PVA, which is known for its water-solubility and the formation of hydrogen bonds with water molecules. The higher the concentration of PSE, the greater the number of available hydrophilic sites, promoting faster water uptake and a higher swelling ratio. Additionally, the initial rapid swelling followed by a plateauing of the swelling ratio suggests that the hydrogel swells quickly when first immersed in water, but this rate slows down as the hydrogel approaches its equilibrium state, where water absorption stabilizes. In short, the hydrophilic nature of PSE, combined with the water-soluble properties of PVA, promotes the swelling effect, and higher concentrations of PSE lead to greater water absorption. These findings suggest that PSE-PVA hydrogels can be customized by adjusting the PSE concentration to meet the specific requirements of various biomedical applications. For example, hydrogels with higher PSE concentrations exhibit enhanced swelling capacity, making them ideal for drug delivery systems that require controlled and sustained release of therapeutic agents. Additionally, their ability to absorb and retain fluids effectively makes them well-suited for use in wound dressings, where maintaining a moist environment is essential for optimal healing.[50]

3.4 *In vitro* antibacterial activity of PSE-PVA composite hydrogels

Fig. 4 presents the antibacterial activity of PSE and the PSE-PVA composite hydrogel against four bacterial strains: *E. coli*, *S. aureus*, *K. pneumoniae*, and *A. baumannii*. Fig. 4A shows images of bacterial growth in response to varying concentrations of PSE (0.25%, 0.50%, and 1%) and PSE-PVA, under both dry and wet conditions. The zone of inhibition defined as the clear area where bacteria cannot grow, increases with higher concentrations of PSE. At the 1.0% concentration, the inhibition zones are significantly larger for all bacterial strains, with *S. aureus* showing the largest zone, indicating a strong antibacterial effect. This suggests that PSE has significant antimicrobial properties, particularly at higher concentrations. The antimicrobial activity of PSE was also evaluated when incorporated into a PVA hydrogel matrix (*i.e.*, PSE-PVA hydrogel). The results show that PSE-PVA formulations, at concentrations of 1%, 0.5%, and 0.25%, retained antibacterial activity in both dry and wet conditions. Fig. 4B provides quantitative data on the zone of inhibition for these formulations, measured in millimeters. A clear trend emerges, with PSE demonstrating greater antibacterial activity, particularly at the 1.0% concentration, which resulted in the largest inhibition zones. For example, the 1.0% PSE-PVA hydrogel produced a maximum inhibition zone of 16 mm ± 0.16% against *K. pneumoniae* in the dry gel form. The differences in inhibition zones between the PSE-PVA groups and the control were statistically significant ($p < 0.05$). This suggests that the PSE-PVA hydrogel enhanced the antibacterial activity of the extract, particularly against *K. pneumoniae*, a common pathogen in hospital-acquired infections. The 1% PSE-PVA hydrogel also showed a 15 mm ± 0.12% inhibition zone against the Gram-positive strain *S. aureus*. However, PSE-PVA consistently demonstrated smaller inhibition zones compared to pure PSE, indicating weaker antibacterial effects. The graph further supports the observation that dry formulations (both PSE and PSE-PVA) produced larger zones of inhibition than wet formulations. Specifically, the antibacterial effect of PSE-PVA was less pronounced at lower concentrations (0.25% and 0.50%), suggesting that the composite hydrogel is less effective than pure PSE in inhibiting bacterial growth. Additionally, the inhibition zones were consistently larger under dry conditions, suggesting that moisture may reduce the antibacterial efficacy of the compounds. These findings suggest that PSE is a more effective antibacterial agent compared to the PSE-PVA composite hydrogel, particularly at higher concentrations and under dry conditions. The antibacterial activity of the PSE-PVA hydrogels was found to be comparable or superior to other natural-extract-based hydrogels reported in recent studies. For example, *Moringa oleifera*-PVA hydrogels

showed formation of zones of inhibition of 11–13 mm against *S. aureus*,[51] while Aloe vera-loaded hydrogels formed zones of inhibition of 9–12 mm against *E. coli* and *P. aeruginosa*.[52] In contrast, the PSE-PVA hydrogel formed inhibition zones of up to 16.5 mm against *E. coli* and 15.2 mm against *S. aureus*, indicating a strong antibacterial profile. The observed antibacterial activity may be attributed not only to the bioactive compounds in PSE but also to potential synergistic effects with the PVA matrix. The PVA network likely supports a sustained release of alkaloids and flavonoids from the hydrogel surface, enhancing bacterial membrane disruption and prolonging contact time, which collectively contribute to stronger antibacterial efficacy. While the dry formulations were more potent, further optimization of the PSE-PVA composite hydrogel could enhance its antibacterial properties for therapeutic use. Overall, the results indicate that the antimicrobial efficacy of the PSE-PVA hydrogel is concentration-dependent and strain-specific. The hydrogel formulation shows promising antibacterial potential, particularly against Gram-negative bacteria. Variations in antimicrobial activity can be attributed to several factors, including the concentration of the plant extract, its incorporation into the hydrogel matrix, and the susceptibility of the bacterial strain. Additionally, the extraction method and specific plant part used may influence the potency of the extract. These findings highlight the potential of the PSE-PVA hydrogel as a novel antibacterial agent, with possible applications in wound healing and infection prevention by reducing microbial load without relying on systemic antibiotics.[53] While the PSE-PVA hydrogel exhibited strong antibacterial activity *in vitro*, this, however, alone does not confirm infection prevention *in vivo*. Future studies involving infected wound models will be necessary to directly assess the ability of the hydrogel to prevent or manage clinical infections.

3.5 Wound appearance and closure, and histological analysis

The wound healing potential of both PSE and PSE-PVA hydrogel was evaluated for 24 days using a murine model, with the animals divided into three groups. The visual presentation of wound appearance and closure is shown in Fig. 5A. The control group displayed minimal healing throughout the experiment. At day 0, the wound size is large, and while some scab formation is visible by day 4 and 14, the wound remains relatively open with only slight closure observed by day 24. In contrast, the animals in the PSE group showed a more noticeable healing trend. Although the wound is still visible at days 4 and 14, there is a clear subsequent reduction in size, with further healing by day 24. The animals in the PSE-PVA group showed the most significant healing, with the wound almost completely closed by day 24 ($p < 0.05$). This group demonstrated rapid healing, with visible closure by day 4 and 14 and substantial reduction in wound size by day 24.

Fig. 5B presents the quantitative measurements of wound size. At day 0, all groups showed similar wound sizes of approximately 8 mm^2. However, by day 4, the animals in the PSE-PVA group showed the greatest reduction in wound size, followed by the PSE group, which also showed significant healing. The animals in the control group showed minimal reduction in wound size, indicating slower healing. This trend continued through days 14 and 24, with the PSE-PVA group exhibiting the smallest wound size, indicating the most effective healing. The PSE group showed a moderate reduction in wound size, while the control group still demonstrated a relatively larger wound size, showing slower healing compared to the treatment groups.

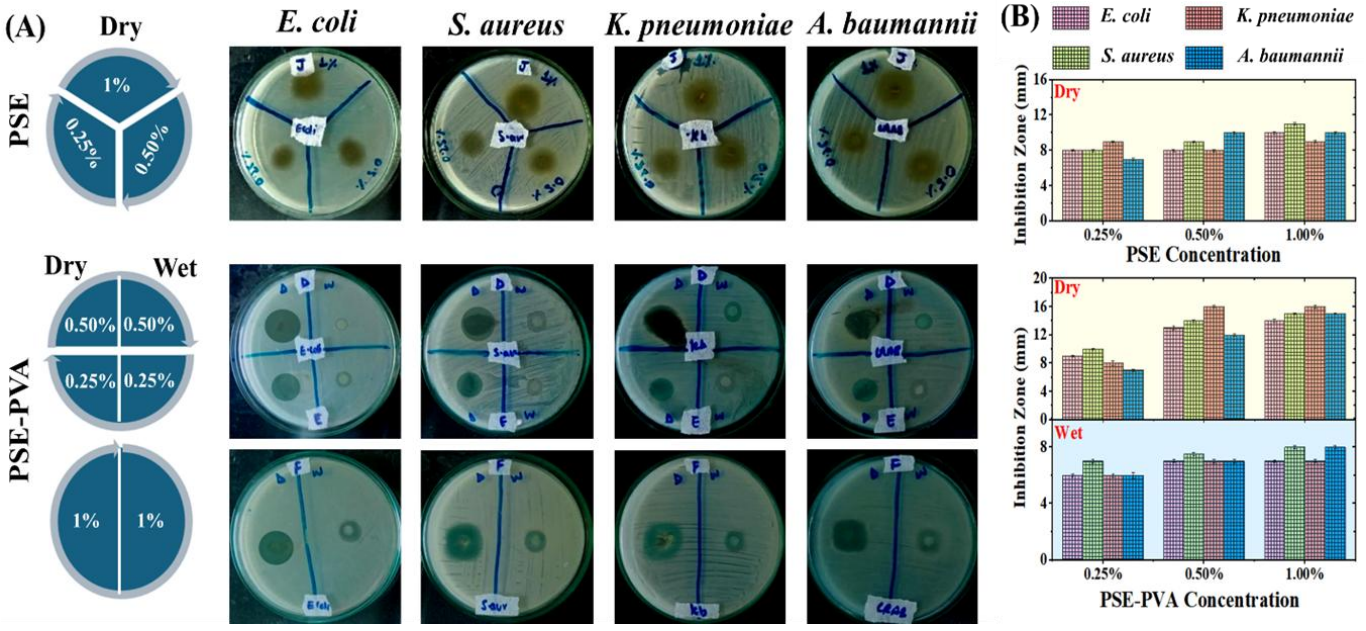

Fig. 4: (A) Visual representation of the zone of inhibition for varying concentrations of *P. somniferum* extract (PSE) and *P. somniferum* extract/polyvinyl alcohol (PSE-PVA) composite gel in both dry and wet states. (B) Quantitative measurement of the zone of inhibition for different concentrations of PSE and PSE/PVA hydrogels.

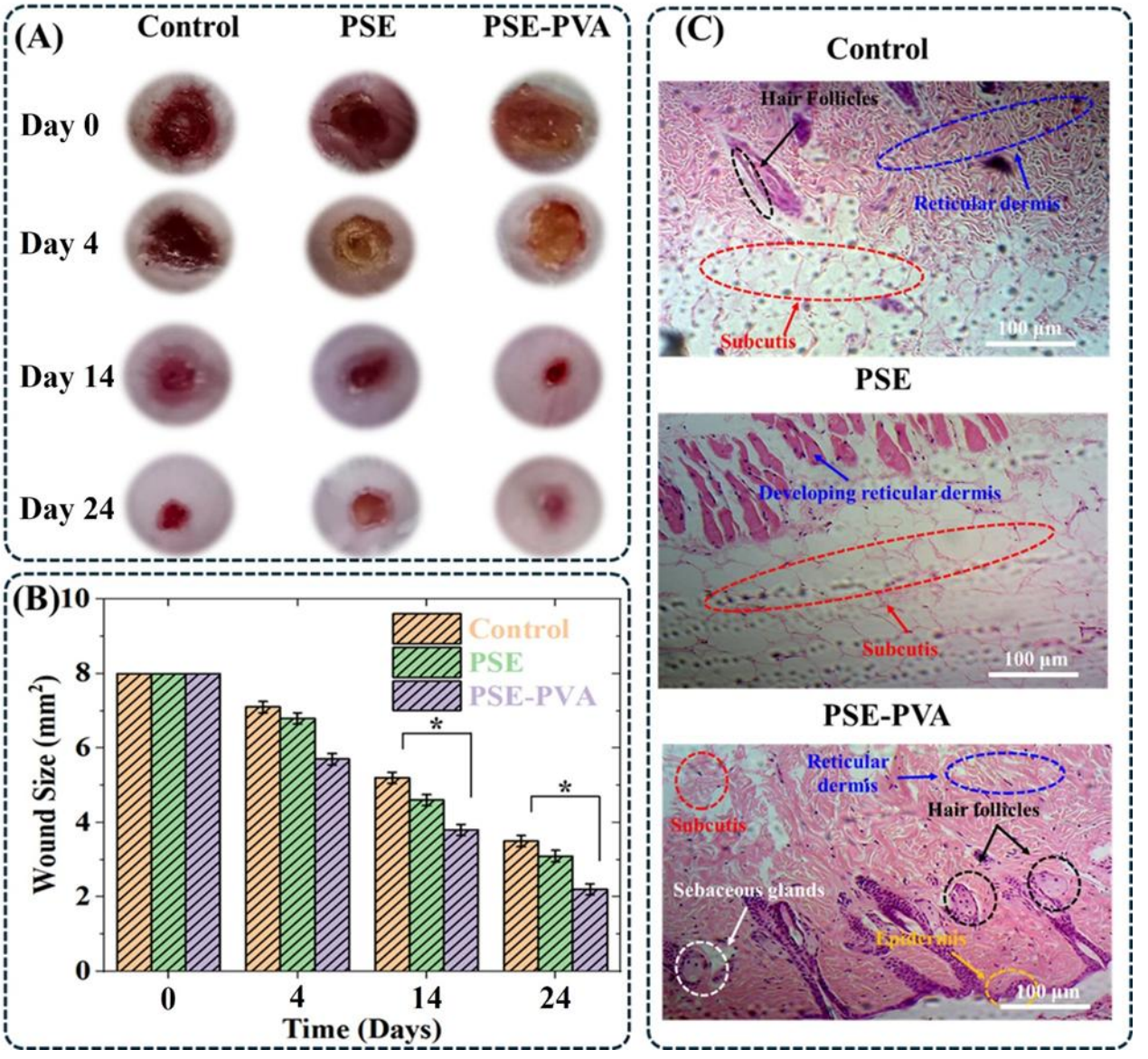

Fig. 5: (A) Visual observation of wound healing in the mice model over time. (B) Quantitative measurements of the wound healing progression for 24 days. Error bars represent SD deviation (n = 3). The difference in wound healing between hydrogel groups was considered significant at $*p < 0.05$. (C) Histological analysis of the control group, PSE group, and PSE/PVA hydrogel group. Black, red, blue, yellow, and white circles show the formation of hair follicles, subcutis, reticular dermis, epidermis, and subcutaneous glands, respectively.

Wound closure was significantly faster in the PSE-PVA-treated group compared to the control and PSE only group ($p < 0.05$). These results indicate that both PSE and PSE-PVA hydrogel have a positive effect on wound healing compared to the control group. The PSE-PVA group demonstrated the most effective healing, suggesting that the combination of PSE with PVA may enhance the wound healing process. This could be due to the improved delivery or sustained release properties of the PSE-PVA formulation, which might facilitate faster tissue repair and regeneration. The PSE group also showed an improvement in wound healing compared to the control, which supports the potential therapeutic role of PSE. However, the healing in the PSE group is slower than in the PSE-PVA group, implying that the formulation with PVA might provide additional benefits. The control group showed minimal healing progression, which highlights the efficacy of the treatment groups (PSE and PSE-PVA) in promoting wound closure. These results align with previous studies that demonstrate the effectiveness of hydrogels in wound healing applications. For example, Li *et al*. highlighted the benefits of hydrogel formulations in promoting cell migration and proliferation, both of which are critical phases in the healing process.[54] Furthermore, incorporating plant extracts, such as PSE, into hydrogels has been shown to enhance their bioactivity and therapeutic effects. One study found that natural compounds in hydrogels not only provided antimicrobial activity but also stimulated fibroblast activity, thereby accelerating wound repair.[55] Additionally, the combination of plant extracts with synthetic polymers like PVA has been documented to produce synergistic effects. A

recent study showed that PVA composite hydrogels improved mechanical properties and moisture retention, both of which are beneficial for wound healing, packaging, and other applications.[56,57] These findings further support the idea that the PSE-PVA hydrogel composition plays a crucial role in enhancing its wound healing efficacy. The superior wound healing potential demonstrated by the PSE-PVA hydrogel in this study is consistent with existing literature, which emphasizes the importance of hydrogel formulations enriched with bioactive compounds for effective wound management. In conclusion, both PSE and PSE-PVA demonstrated promising effects on wound healing, with the PSE-PVA formulation showing superior results. We will explore the mechanism behind the enhanced healing in the PSE-PVA group, as well as optimize the formulations for even better therapeutic outcomes in wound care in our future studies.

The effectiveness of PSE and PSE-PVA hydrogel in wound healing and closure was assessed through histological examination of the different animal treatment groups. The histological findings for each group were compared with the control, as shown in Fig. 5C, providing valuable insights into the wound healing progress and tissue regeneration across various treatments. The histological analysis of the tissue sections from the Control, PSE, and PSE/PVA hydrogel groups revealed important differences in skin structure following treatment (Fig. 5C). The optical microscopic images of the histology clearly showed no wound healing. The area remained in an inflammatory state, and no evidence of the formation of the subcutaneous, dermal, or epidermal layers was observed. This indicates that the control group exhibited limited wound healing, highlighting the necessity of effective treatment to accelerate the healing process. In contrast, Group 2, which was treated with PSE, also demonstrated incomplete wound healing after two weeks. While some improvement was noted, the regenerative process of the skin was still insufficient. Notably, the wound site lacked the development of key skin structures, including sebaceous glands, hair follicles, and the epidermal layer, indicating that PSE treatment alone did not fully support the regeneration of complex skin tissues within the given timeframe. Group 3, which received the PSE-PVA hydrogel treatment, showed the most promising results. Within just one week of treatment, significant improvement was observed in the healing process of the skin. The histological image shows the rapid regeneration of the epidermal layer, the formation of new hair follicles, and the development of sebaceous glands. These observations suggest that the PSE-PVA hydrogel not only accelerated the wound healing process but also promoted the regeneration of essential skin structures, providing a more complete recovery compared to the PSE treatment alone. The epidermal layer, which serves as the first line of defense in skin regeneration, was notably formed within one to two days in this group, a clear indication of the superior performance of the PSE-PVA hydrogel. In conclusion, the PSE/PVA hydrogel demonstrated a strong potential for promoting skin regeneration. The formation of sebaceous glands and changes in epidermal and dermal structures indicate that the hydrogel could be a promising candidate for enhancing tissue differentiation and supporting wound healing processes. These findings are in accordance with the well-explored pharmacological properties, including analgesic, antibacterial, antipyretic, and anti-inflammatory effects of *P. somniferum*.[18,58] These properties make *P. somniferum* a valuable candidate in wound healing applications. Traditionally, the medicinal uses of *P. somniferum*, primarily for sedative analgesics, cough treatment, and diarrhea management, are well documented.[59] However, it is essential to recognize that *P. somniferum* contains alkaloids such as codeine and thebaine, which may have detrimental effects on wound healing and overall health if misused. Therefore, while *P. somniferum* demonstrates promising therapeutic potential; further studies are needed to fully understand its bioactive compounds' influence on wound healing. Moreover, optimizing its use in therapeutic applications to ensure safety and efficacy remains a critical area for future research.

4. Conclusion

This study successfully developed a bioactive hydrogel composed of *P. somniferum* extract (PSE) and polyvinyl alcohol (PVA) for wound healing applications. The unique structure of hydrogel, characterized by smoother and more organized textures, suggests its suitability for promoting cell growth and tissue regeneration. The high swelling behavior of hydrogel is crucial for maintaining a moist wound environment that enhances healing. The PSE-PVA hydrogel displayed strong antibacterial activity against common wound-associated pathogens, demonstrating its potential in preventing infection at the wound site. *In vivo* studies confirmed the promising therapeutic effects of the hydrogel, with a 95% reduction in wound size in 24 days. Histological analysis further supported these findings, showing rapid epidermal regeneration, early formation of new hair follicles, and sebaceous glands, which are indicative of effective tissue repair and regeneration. Overall, the *P. somniferum* extract-loaded polyvinyl alcohol hydrogel holds strong potential for clinical applications in wound healing, offering advantages such as controlled drug release, infection prevention, and enhanced tissue regeneration. With further optimization and investigation of *in vivo* release profiles of bioactive molecules and toxicity analysis, this hydrogel could significantly improve therapeutic outcomes in wound care and other related medical applications. Future studies will focus on translational steps, including hydrogel scale-up, regulatory compliance, and comprehensive assessment of long-term stability, degradation behavior, drug release kinetics, and *in vitro* cytotoxicity to establish the clinical applicability and biocompatibility of the formulation. Additionally, long-term storage stability and shelf life under different environmental conditions will be evaluated to ensure practical usability.

Acknowledgments
This research was supported by the Metasequoia Teacher Research Start-up Fund, Nanjing Forestry University, Nanjing, China (163105998, 163105999). The authors gratefully acknowledge the scientific support provided by the UNESCO Chair on Science and Innovation for Environmental Sustainability at Dhofar University, Salalah, Oman.

Conflict of Interest
The authors declare that they have no known competing financial interests or personal relationships that could have appeared to influence the work reported in this paper.

Ethical Approval
All methods were accomplished consistently with the pertinent guidelines and regulations, and the experiments with animal models were in line with standard guidelines. The experimental design for experimental animal use was approved by the local Biosafety and Bioethics Committee at the National University of science and technology, Islamabad, Pakistan. We hereby confirm that the study is reported in accordance with ARRIVE guidelines (https://arriveguidelines.org). The principles of replacement, reduction, and refinement (the 3Rs) were followed

Supporting Information
Not applicable.

CRediT Statement
Faiza Tariq: Conceptualization, Data curation, Formal analysis, Writing – Original draft. **Adeeb Shehzad:** Conceptualization, Supervision, Writing – Review & editing. **Mazhar Ul-Islam:** Conceptualization, Writing – Review & editing. **Abdullah Al-Saidi:** Data curation, Writing – Review & editing. **Sehrish Manan:** Data curation, Methodology, Funding acquisition. **Fazli Subhan:** Data curation, Methodology. **Fanar Hamad Alshammari:** Data curation, Methodology. **Guang Yang:** Conceptualization, Supervision, Writing – Review & editing. **Muhammad Wajid Ullah:** Conceptualization, Supervision, Funding acquisition, Writing – Review & editing.

References
[1] O. A. Peña, P. Martin, Cellular and molecular mechanisms of skin wound healing, *Nature Reviews Molecular Cell Biology*, 2024, **25**, 599-616, doi: 10.1038/s41580-024-00715-1.
[2] S. Kalidas, S. Sumathi, Biomedical application of gelatin-PVA-silk fibre composite reinforced with copper and manganese substituted hydroxyapatite, *Journal of Materials Research and Technology*, 2025, **34**, 1850-1864, doi: 10.1016/j.jmrt.2024.12.162.
[3] E. M. Tottoli, R. Dorati, I. Genta, E. Chiesa, S. Pisani, B. Conti, Skin wound healing process and new emerging technologies for skin wound care and regeneration, *Pharmaceutics*, 2020, **12**, 735, doi: 10.3390/pharmaceutics12080735.
[4] L. Mao, L. Wang, M. Zhang, M. W. Ullah, L. Liu, W. Zhao, Y. Li, A. A. Q. Ahmed, H. Cheng, Z. Shi, G. Yang, *In situ* synthesized selenium nanoparticles-decorated bacterial cellulose/gelatin hydrogel with enhanced antibacterial, antioxidant, and anti-inflammatory capabilities for facilitating skin wound healing, *Advanced Healthcare Materials*, 2021, **10**, 2100402, doi: 10.1002/adhm.202100402.
[5] T. Huang, Y. Ma, H. Chen, S. Zhang, L. Liu, M. Chen, R. Jia, L. Lin, M. W. Ullah, Y. Fan, A silk nanofiber and hyaluronic acid composite hemostatic sponge for compressible hemostasis, *International Journal of Biological Macromolecules*, 2025, **307**, 142262, doi: 10.1016/j.ijbiomac.2025.142262.
[6] S. Yue, S. Wang, D. Han, S. Huang, L. Sun, M. Xiao, Y. Meng, Polyvinyl alcohol/montmorillonite nanocomposite coated biodegradable films with outstanding barrier properties, *ES Materials & Manufacturing*, 2023, **20**, 834, doi: 10.30919/esmm5f834.
[7] M. Bhat, M. R. Abhilash, S. V. Mamatha, S. Das, G. Roymahapatra, Photocatalytic degradation of dyes by titania/ferric oxide/polyvinyl alcohol nanocomposites, *ES General*, 2023, **2**, 981, doi: 10.30919/esg981.
[8] M. Deptuła, J. Zieliński, A. Wardowska, M. Pikuła, Wound healing complications in oncological patients: perspectives for cellular therapy, *Advances in Dermatology and Allergology*, 2019, **36**, 139-146, doi: 10.5114/ada.2018.72585.
[9] C. Shi, C. Wang, H. Liu, Q. Li, R. Li, Y. Zhang, Y. Liu, Y. Shao, J. Wang, Selection of appropriate wound dressing for various wounds, *Frontiers in Bioengineering and Biotechnology*, 2020, **8**, 182, doi: 10.3389/fbioe.2020.00182.
[10] M. Akrami-Hasan-Kohal, L. Tayebi, M. Ghorbani, Curcumin-loaded naturally-based nanofibers as active wound dressing mats: morphology, drug release, cell proliferation, and cell adhesion studies, *New Journal of Chemistry*, 2020, **44**, 10343-10351, doi: 10.1039/d0nj01594f.
[11] W. Sajjad, F. He, M. W. Ullah, M. Ikram, S. M. Shah, R. Khan, T. Khan, A. Khalid, G. Yang, F. Wahid, Fabrication of bacterial cellulose-curcumin nanocomposite as a novel dressing for partial thickness skin burn, *Frontiers in Bioengineering and Biotechnology*, 2020, **8**, 553037, doi: 10.3389/fbioe.2020.553037.
[12] R. Yu, H. Zhang, B. Guo, Conductive biomaterials as bioactive wound dressing for wound healing and skin tissue engineering, *Nano-Micro Letters*, 2022, **14**, doi: 10.1007/s40820-021-00751-y.
[13] W. Zhang, L. Liu, H. Cheng, J. Zhu, X. Li, S. Ye, X. Li, Hydrogel-based dressings designed to facilitate wound healing, *Materials Advances*, 2024, **5**, 1364-1394, doi: 10.1039/d3ma00682d.
[14] Z. Ji, T. Wei, J. Zhu, J. Hu, Z. Xiao, B. Bai, X. Lv, Y. Miao, M. Chen, C. Wang, F. Pan, Y. Yang, M. Li, Q. Chen, Actively contractible and antibacterial hydrogel for accelerated wound healing, *Nano Research*, 2024, **17**, 7394-7403, doi: 10.1007/s12274-024-6674-6.
[15] L. Zhang, Y. Wang, M. Yang, W. Yu, Z. Zhao, Y. Liu, An injectable, self-healing, adhesive multifunctional hydrogel promotes bacteria-infected wound healing, *Polymers*, 2024, **16**,

1316, doi: 10.3390/polym16101316.
[16] M. Zhang, C. Zhu, Dynamic hydrogels against infections: from design to applications, *Gels*, 2024, **10**, 331, doi: 10.3390/gels10050331.
[17] J. Zhu, H. Cheng, Z. Zhang, K. Chen, Q. Zhang, C. Zhang, W. Gao, Y. Zheng, Antibacterial hydrogels for wound dressing applications: current status, progress, challenges, and trends, *Gels*, 2024, **10**, 495, doi: 10.3390/gels10080495.
[18] X. Liang, H.-J. Zhong, H. Ding, B. Yu, X. Ma, X. Liu, C.-M. Chong, J. He, Polyvinyl alcohol (PVA)-based hydrogels: recent progress in fabrication, properties, and multifunctional applications, *Polymers*, 2024, **16**, 2755, doi: 10.3390/polym16192755.
[19] X. Li, X. Ji, K. Chen, M. W. Ullah, X. Yuan, Z. Lei, J. Cao, J. Xiao, G. Yang, Development of finasteride/PHBV@polyvinyl alcohol/chitosan reservoir-type microspheres as a potential embolic agent: from *in vitro* evaluation to animal study, *Biomaterials Science*, 2020, **8**, 2797-2813, doi: 10.1039/c9bm01775e.
[20] A. S. Oliveira, O. Seidi, N. Ribeiro, R. Colaço, A. P. Serro, Tribomechanical comparison between PVA hydrogels obtained using different processing conditions and human cartilage, *Materials*, 2019, **12**, 3413, doi: 10.3390/ma12203413.
[21] X. Li, X. Ji, K. Chen, X. Yuan, Z. Lei, M. W. Ullah, J. Xiao, G. Yang, Preparation and evaluation of ion-exchange porous polyvinyl alcohol microspheres as a potential drug delivery embolization system, *Materials Science and Engineering: C*, 2021, **121**, 111889, doi: 10.1016/j.msec.2021.111889.
[22] X. Li, B. Li, M. W. Ullah, R. Panday, J. Cao, Q. Li, Y. Zhang, L. Wang, G. Yang, Water-stable and finasteride-loaded polyvinyl alcohol nanofibrous particles with sustained drug release for improved prostatic artery embolization: *in vitro* and *in vivo* evaluation, *Materials Science and Engineering: C*, 2020, **115**, 111107, doi: 10.1016/j.msec.2020.111107.
[23] Z. Özbaş, B. Özkahraman, G. Bayrak, A. Kılıç Süloğlu, I. Perçin, F. Boran, E. Tamahkar, Poly(vinyl alcohol)/(hyaluronic acid-g-kappa-carrageenan) hydrogel as antibiotic-releasing wound dressing, *Chemical Papers*, 2021, **75**, 6591-6600, doi: 10.1007/s11696-021-01824-3.
[24] D. Jessy Mercy, A. Thirumalai, S. Udayakumar, B. Deepika, G. Janani, A. Girigoswami, K. Girigoswami, Enhancing wound healing with nanohydrogel-entrapped plant extracts and nanosilver: an *in vitro* investigation, *Molecules*, 2024, **29**, 5004, doi: 10.3390/molecules29215004.
[25] A. I. Lopes, M. M. Pintado, F. K. Tavaria, Plant-based films and hydrogels for wound healing, *Microorganisms*, 2024, **12**, 438, doi: 10.3390/microorganisms12030438.
[26] E. Muscolino, A. B. Di Stefano, M. Trapani, M. A. Sabatino, D. Giacomazza, F. Moschella, A. Cordova, F. Toia and C. Dispenza, Injectable xyloglucan hydrogels incorporating spheroids of adipose stem cells for bone and cartilage regeneration, *Materials Science and Engineering: C*, 2021, **131**, 112545, doi: 10.1016/j.msec.2021.112545.
[27] A. Fatima, S. Yasir, M. Ul-Islam, T. Kamal, Md. W. Ahmad, Y. Abbas, S. Manan, M. W. Ullah and G. Yang, Ex situ development and characterization of green antibacterial bacterial cellulose-based composites for potential biomedical applications, *Advanced Composites and Hybrid Materials*, 2022, **5**, 307–321, doi: 10.1007/s42114-021-00369-z.
[28] R. S. R. Machado, V. Bonhomme, R. Soteras, A. Jeanty, L. Bouby, A. Evin, M. J. Fernandes Martins, S. Gonçalves, F. Antolín, A. Salavert, H. R. Oliveira, The origins and spread of the opium poppy (*Papaver somniferum*L.) revealed by genomics and seed morphometrics, *Philosophical Transactions of the Royal Society B: Biological Sciences*, 2025, **380**, 20240198, doi: 10.1098/rstb.2024.0198.
[29] A. Fatima, S. Yasir, M. S. Khan, S. Manan, M. W. Ullah, M. Ul-Islam, Plant extract-loaded bacterial cellulose composite membrane for potential biomedical applications, *Journal of Bioresources and Bioproducts*, 2021, **6**, 26-32, doi: 10.1016/j.jobab.2020.11.002.
[30] A. Fatima, M. Ul-Islam, S. Yasir, S. Khan, S. Manan, A. Shehzad, M. W. Ahmad, R. Al-Shannaq, S. U. Islam, Y. Abbas, F. Subhan, A. A. A. Sabour, M. A. Alshiekheid, M. W. Ullah, *Ex situ* fabrication and bioactivity characterization of Neem and Sage-infused bacterial cellulose membranes for sustainable antimicrobial applications, *International Journal of Biological Macromolecules*, 2025, **287**, 138433, doi: 10.1016/j.ijbiomac.2024.138433.
[31] P. Májer, É. Z. Németh, Alkaloid accumulation and distribution within the capsules of two opium poppy (*Papaver somniferum* L.) varieties, *Plants*, 2024, **13**, 1640, doi: 10.3390/plants13121640.
[32] D. B. Ozdemir, A. Karayigit, E. Tekin, E. Kocaturk, C. Bal, I. Ozer, The effect of local papaverine use in an experimental high-risk colonic anastomosis model: reduced inflammatory findings and less necrosis, *Journal of Clinical Medicine*, 2024, **13**, 5638, doi: 10.3390/jcm13185638.
[33] S. Aalinezhad, F. Dabaghian, A. Namdari, M. Akaberi, S. Ahmad Emami, Phytochemistry and pharmacology of alkaloids from papaver spp. a structure–activity based study, *Phytochemistry Reviews*, 2025, **24**, 585-657, doi: 10.1007/s11101-024-09943-x.
[34] K. Snelson, A. Downe, Use of topical morphine gel in epidermolysis bullosa wounds: a series of case studies, *International Wound Journal*, 2023, **20**, 1954-1959, doi: 10.1111/iwj.14055.
[35] H. Yu, D. Chen, W. Lu, C. Zhang, H. Wang, Z. Peng, H. Jiang, C. Xiao, Characterization of polyvinyl alcohol/chitosan nanofibers loaded with royal jelly by blending electrospinning for potential wound dressings, *International Journal of Biological Macromolecules*, 2025, **307**, 141977, doi: 10.1016/j.ijbiomac.2025.141977.
[36] A. Eskandarinia, M. H. Morowvat, S. V. Niknezhad, M. A. Baghbadorani, M. Michálek, S. Chen, M. M. Nemati, M. Negahdaripour, R. Heidari, A. Azadi, Y. Ghasemi, A photocrosslinkable and hemostatic bilayer wound dressing based on gelatin methacrylate hydrogel and polyvinyl alcohol foam for

skin regeneration, *International Journal of Biological Macromolecules*, 2024, **266**, 131231, doi: 10.1016/j.ijbiomac.2024.131231.
[37] A. Ali Kadhim, N. R. Abbas, H. H. Kadhum, S. Albukhaty, M. S. Jabir, A. M. Naji, S. S. Hamzah, M. K. A. Mohammed, H. Al-Karagoly, Investigating the effects of biogenic zinc oxide nanoparticles produced using *Papaver somniferum* extract on oxidative stress, cytotoxicity, and the induction of apoptosis in the THP-1 cell line, *Biological Trace Element Research*, 2023, **201**, 4697-4709, doi: 10.1007/s12011-023-03574-7.
[38] B. M. Bakadia, B. O. O. Boni, A. A. Q. Ahmed, R. Zheng, Z. Shi, M. W. Ullah, L. Lamboni, G. Yang, *In situ* synthesized porous bacterial cellulose/poly(vinyl alcohol)-based silk sericin and azithromycin release system for treating chronic wound biofilm, *Macromolecular Bioscience*, 2022, **22**, 2200201, doi: 10.1002/mabi.202200201.
[39] L. Chen, Z. Tian and Y. Du, Synthesis and pH sensitivity of carboxymethyl chitosan-based polyampholyte hydrogels for protein carrier matrices, *Biomaterials*, 2004, **25**, 3725–3732. doi: 10.1016/j.biomaterials.2003.09.100.
[40] M. Liao, Y. Zhao, Y. Pan, J. Pan, Q. Yao, S. Zhang, H. Zhao, Y. Hu, W. Zheng, W. Zhou, X. Dong, A good adhesion and antibacterial double-network composite hydrogel from PVA, sodium alginate and tannic acid by chemical and physical cross-linking for wound dressings, *Journal of Materials Science*, 2023, **58**, 5756-5772, doi: 10.1007/s10853-023-08378-7.
[41] S. Kamel, S. Dacrory, P. Hesemann, N. Bettache, L. M. A. Ali, L. Postel, E. M. Akl, M. El-Sakhawy, Wound dressings based on sodium alginate–polyvinyl alcohol–moringa oleifera extracts, *Pharmaceutics*, 2023, **15**, 1270, doi: 10.3390/pharmaceutics15041270.
[42] Y. Wu, C. Yan, Y. Wang, C. Gao, Y. Liu, Biomimetic structure of chitosan reinforced epoxy natural rubber with self-healed, recyclable and antimicrobial ability, *International Journal of Biological Macromolecules*, 2021, **184**, 9-19, doi: 10.1016/j.ijbiomac.2021.06.037.
[43] M. J. Ahmed, B. H. Hameed, E. H. Hummadi, Review on recent progress in chitosan/chitin-carbonaceous material composites for the adsorption of water pollutants, *Carbohydrate Polymers*, 2020, **247**, 116690, doi: 10.1016/j.carbpol.2020.116690.
[44] P. Wongsa, P. Phatikulrungsun, S. Prathumthong, FT-IR characteristics, phenolic profiles and inhibitory potential against digestive enzymes of 25 herbal infusions, *Scientific Reports*, 2022, **12**, 6631, doi: 10.1038/s41598-022-10669-z.
[45] S. Wang, N. Wang, J. Xu, X. Zhang, S. Dou, Contribution of microbial residues obtained from lignin and cellulose on humus formation, *Sustainability*, 2019, **11**, 4777, doi: 10.3390/su11174777.
[46] R. H. Ellerbrock, H. H. Gerke, FTIR spectral band shifts explained by OM–cation interactions, *Journal of Plant Nutrition and Soil Science*, 2021, **184**, 388-397, doi: 10.1002/jpln.202100056.
[47] T.-J. Jiang, H. M. Morgan Jr, W.-T. Tsai, H. Chien, T.-B. Yen, Y.-R. Lee, Thermochemical conversion of biomass into biochar: enhancing adsorption kinetics and pore properties for environmental sustainability, *Sustainability*, 2024, **16**, 6623, doi: 10.3390/su16156623.
[48] M. Fan, D. Dai, B. Huang, Fourier transform infrared spectroscopy for natural fibres, *Fourier Transform - Materials Analysis*, IntechOpen, London, 2012 doi: 10.5772/35482.
[49] M. Barbălată-Mândru, D. Serbezeanu, M. Butnaru, C. M. Rîmbu, A. A. Enache, M. Aflori, Poly(vinyl alcohol)/plant extracts films: preparation, surface characterization and antibacterial studies against gram positive and gram negative bacteria, *Materials*, 2022, **15**, 2493, doi: 10.3390/ma15072493.
[50] F. Rashid, S. S. Soshi, M. A. Gafur, Development and characterization of hybrid film made of hydroxyapatite, poly vinyl alcohol and gelatin for biomedical application, *Materials Sciences and Applications*, 2024, **15**, 320-335, doi: 10.4236/msa.2024.159022.
[51] G. W. Tyson, J. Chapman, P. Hugenholtz, E. E. Allen, R. J. Ram, P. M. Richardson, V. V. Solovyev, E. M. Rubin, D. S. Rokhsar, J. F. Banfield, Community structure and metabolism through reconstruction of microbial genomes from the environment, *Nature*, 2004, **428**, 37-43, doi: 10.1038/nature02340.
[52] H. D. Kabiru, K. B. Ahmad, N. M. Bello and S. O. Paul, Formulation and evaluation of in vitro antioxidant and antimicrobial activities of herbal hydrogel loaded with Moringa oleifera leaf extract, *Science World Journal*, 2023, **18**, 101–105.
[53] H. Khanzada, A. Salam, M. B. Qadir, D.-N. Phan, T. Hassan, M. U. Munir, K. Pasha, N. Hassan, M. Q. Khan, I. S. Kim, Fabrication of promising antimicrobial aloe vera/PVA electrospun nanofibers for protective clothing, *Materials*, 2020, **13**, 3884, doi: 10.3390/ma13173884.
[54] T. Li, W. Sun, D. Qian, P. Wang, X. Liu, C. He, T. Chang, G. Liao and J. Zhang, Plant-derived biomass-based hydrogels for biomedical applications, *Trends in Biotechnology*, 2025, **43**, 802-811, doi: 10.1016/j.tibtech.2024.09.010.
[55] K. Nuutila, E. Eriksson, Moist wound healing with commonly available dressings, *Advances in Wound Care*, 2021, **10**, 685-698, doi: 10.1089/wound.2020.1232.
[56] O. Kapusta, A. Jarosz, K. Stadnik, D. A. Giannakoudakis, B. Barczyński, M. Barczak, Antimicrobial natural hydrogels in biomedicine: properties, applications, and challenges: a concise review, *International Journal of Molecular Sciences*, 2023, **24**, 2191, doi: 10.3390/ijms24032191.
[57] Y. Zhang, Y. Wang, Y. Li, Y. Yang, M. Jin, X. Lin, Z. Zhuang, K. Guo, T. Zhang, W. Tan, Application of collagen-based hydrogel in skin wound healing, *Gels*, 2023, **9**, 185, doi: 10.3390/gels9030185.
[58] Y. Zhong, Q. Lin, H. Yu, L. Shao, X. Cui, Q. Pang, Y. Zhu, R. Hou, Construction methods and biomedical applications of PVA-based hydrogels, *Frontiers in Chemistry*, 2024, **12**, 1376799, doi: 10.3389/fchem.2024.1376799.
[59] I. Stranska, M. Skalicky, J. Novak, E. Matyasova, V. Hejnak, Analysis of selected poppy (*Papaver somniferum* L.) cultivars:

Pharmaceutically important alkaloids, *Industrial Crops and Products*, 2013, **41**, 120-126, doi: 10.1016/j.indcrop.2012.04.018.